PAPER

Insertion/Deletion/Substitution Error Correction by a Modified Successive Cancellation Decoding of Polar Code*

Hikari KOREMURA[†], *Nonmember and* **Haruhiko KANEKO**[†a)], *Member*

SUMMARY This paper presents a successive cancellation (SC) decoding of polar codes modified for insertion/deletion/substitution (IDS) error channels, in which insertions and deletions are described by drift values. The recursive calculation of the original SC decoding is modified to include the drift values as stochastic variables. The computational complexity of the modified SC decoding is $O(D^3)$ with respect to the maximum drift value D, and $O(N \log N)$ with respect to the code length N. The symmetric capacity of polar bit channel is estimated by computer simulations, and frozen bits are determined according to the estimated symmetric capacity. Simulation results show that the decoded error rate of polar code with the modified SC list decoding is lower than that of existing IDS error correction codes, such as marker-based code and spatially-coupled code.

key words: *insertion error, deletion error, synchronization error, polar code, successive cancellation decoding, list decoding*

1. Introduction

Synchronization errors will be a major obstacle to improve the reliability of some types of future high-density memory and storage devices, such as, bit-patterned media recording [1], racetrack memory [2], [3], and DNA archival storage [4]. Hence, it is expected that error control codes capable of correcting synchronization errors will be crucial to improve the reliability of these devices. Channels with synchronization errors are usually modeled by insertion/deletion/substitution (IDS) channel, and several classes of IDS error correcting codes were proposed. For example, codes with the bounded distance decoding were designed based on a constraint on weighted sum of codeword bits, such as, single IDS error correcting code [5], multiple IDS error correcting code [6], and non-binary single IDS error correcting code [7]. Another strategy for IDS error correction is to employ the concatenated coding, where the outer code is a random error correcting code (e.g., LDPC code), and the inner code controls prior probabilities of channel input bits, such as watermark embedding [8] and marker insertion [9]. Also, it was shown that spatially-coupled codes can correct IDS errors without using the inner coding [10].

Arıkan proposed polar coding with successive cancellation (SC) decoding [11], which can achieve the symmetric capacity of any binary-input memoryless channel with the computational complexity of $O(N \log N)$, where $N = 2^n$ is the code length. Şaşoğlu et al. proved that the polar code can achieve the capacity of any discrete memoryless channel [12]. To improve the performance of polar code with finite code length, Tal and Vardy presented SC list (SCL) decoding with cyclic redundancy check (CRC) [13]. For correction of synchronization errors using the polar code, Thomas et al. presented a polar coding for channels with erasures and deletions [14], where the coding mainly deals with single deletion errors. Tian et al. proposed an SC decoding of polar code for channels with d deletions [15], and they proved that this coding achieves the symmetric capacity.

Existing IDS channels often assume that insertions and deletions occur probabilistically [3], [4], [8]–[10], as opposed to the deletion model in [15]. That is, received word may have multiple insertion and deletion errors simultaneously, and thus the numbers of insertions and deletions cannot be determined uniquely from the received word length N'. Hence, extension of the d-deletion correction polar coding [15] to the multiple insertion/deletion error correction coding will not be straightforward. From this, we present an SC decoding of polar codes for IDS channels in which insertion, deletion, and substitution errors occur with probability p_i, p_d, and p_s, respectively, under a constraint on maximum drift between transmitted and received bits. This paper employs an IDS channel model expressed by a sequence of drift values, which is suitable for deriving a modified recursive computation in the SC decoding. That is, the appropriate combination of the IDS channel model and recursive computation enables a natural extension of the existing SC decoding to IDS error correction. Simulation results show that the presented SC decoding has lower decoded error rates compared to the existing marker-based code and spatially-coupled code.

The rest of this paper is organized as follows. Section 2 describes notations used in this paper. Section 3 defines IDS channel model. Section 4 presents a polar coding with modified SC decoding for IDS channel. Section 5 shows simulation results, and Sect. 6 concludes this paper.

2. Notations

This paper uses the following notations. Finite subsets of integers are defined as $\mathbb{Z}_M = \{0, 1, \ldots, M-1\}$ and $\mathbb{B} = \mathbb{Z}_2 = \{0, 1\}$. The inversion of bit x is denoted as $\overline{x} = x \oplus 1$, where $\oplus$ is the XOR operator, and $x, \overline{x} \in \mathbb{B}$. For a binary vector $\boldsymbol{a} = (a_0, a_1, \ldots, a_{N-1}) \in \mathbb{B}^N$ of length N, sub-vector $\boldsymbol{a}_i^j$ is defined as

Manuscript received June 3, 2019.
Manuscript revised November 13, 2019.

[†]The authors are with the School of Computing, Tokyo Institute of Technology, Tokyo, 152-8552 Japan.

*Some parts of this paper were presented at the 2019 IEEE International Symposium on Information Theory (ISIT 2019).

a) E-mail: hkaneko@ieee.org

DOI: 10.1587/transfun.2019EAP1079

$$\boldsymbol{a}_i^j = \begin{cases} (a_i, a_{i+1}, \ldots, a_j) & (0 \le i \le j \le N-1) \\ \varepsilon & (\text{otherwise}) \end{cases},$$

where ε is the vector of length zero. For a binary vector $\boldsymbol{a} = (a_0, a_1, \ldots, a_{2N-1}) \in \mathbb{B}^{2N}$ of even-length $2N$, mappings even($\boldsymbol{a}$) and odd($\boldsymbol{a}$) are defined as follows:

$$\begin{aligned} \text{even}\,(\boldsymbol{a}) &= (a_0, a_2, \ldots, a_{2i}, \quad \ldots, a_{2N-2}), \\ \text{odd}\,(\boldsymbol{a}) &= (a_1, a_3, \ldots, a_{2i+1}, \ldots, a_{2N-1}). \end{aligned}$$

For two binary vectors, $\boldsymbol{a} = (a_0, a_1, \ldots, a_{N-1}) \in \mathbb{B}^N$ and $\boldsymbol{b} = (b_0, b_1, \ldots, b_{N-1}) \in \mathbb{B}^N$, XOR of $\boldsymbol{a}$ and $\boldsymbol{b}$ is defined as

$$\boldsymbol{a} \oplus \boldsymbol{b} = (a_0 \oplus b_0, a_1 \oplus b_1, \ldots, a_{N-1} \oplus b_{N-1}).$$

Probability that a random variable X takes a value x is simply denoted as $p(x) \triangleq \Pr(X = x)$. Conditional and joint probabilities are denoted similarly, that is, $p(x|y) \triangleq \Pr(X = x|Y = y)$ and $p(x, y) \triangleq \Pr(X = x, Y = y)$.

3. Channel Model

Let $\boldsymbol{x}$ and $\boldsymbol{y}$ be transmitted and received words, respectively, where the words are expressed by binary vectors as

$$\begin{aligned} &\boldsymbol{x} = \boldsymbol{x}_0^{N-1} = (x_0, x_1, \ldots, x_{N-1}) \in \mathbb{B}^N \quad \text{and} \\ &\boldsymbol{y} = \boldsymbol{y}_0^{N'-1} = (y_0, y_1, \ldots, y_{N'-1}) \in \mathbb{B}^{N'}. \end{aligned}$$

Let p_i, p_d, and p_s be insertion, deletion, and substitution error probabilities, respectively. And let D be the maximum absolute value of drift between $\boldsymbol{x}$ and $\boldsymbol{y}$. Insertion/deletion errors between $\boldsymbol{x}$ and $\boldsymbol{y}$ are expressed by a drift vector

$$\boldsymbol{d} = (d_0, d_1, \ldots, d_{N-1}, d_N) \in \mathcal{D}^{N+1},$$

where $\mathcal{D} = \{-D, \ldots, -1, 0, 1, \ldots, D\}$ is the set of drift values. We assume that the drift vector is determined by Markov process with the following state transition probabilities:

$$p(d_{i+1}|d_i) = \begin{cases} p_\text{i} & ((d_{i+1} = d_i + 1) \wedge (d_i \ne D)) \\ p_\text{d} & ((d_{i+1} = d_i - 1) \wedge (d_i \ne -D)) \\ 1 - p_\text{i} - p_\text{d} & ((d_{i+1} = d_i) \wedge (-D < d_i < D)) \\ 1 - p_\text{i} & ((d_{i+1} = d_i) \wedge (d_i = -D)) \\ 1 - p_\text{d} & ((d_{i+1} = d_i) \wedge (d_i = D)) \\ 0 & (\text{otherwise}) \end{cases}, \quad (1)$$

where the initial drift value is $d_0 = 0$. Figure 1 (a) shows the state transition diagram of d_i. From this definition, $\boldsymbol{d}$ satisfies $-1 \le d_{i+1} - d_i \le 1$ for all $i \in \mathbb{Z}_N$. Let $\mathcal{I}(i; d_i, d_{i+1})$ be a set of indices in received word $\boldsymbol{y}_0^{N'-1}$ corresponding to the i-th transmitted bit x_i, that is,

$$\mathcal{I}(i; d_i, d_{i+1}) = \{i' \,|\, i + d_i \le i' < (i+1) + d_{i+1}\} \subset \mathbb{Z}_{N'},$$

where $N' = N + d_N$. The following relations hold for $\mathcal{I}(i; d_i, d_{i+1})$:

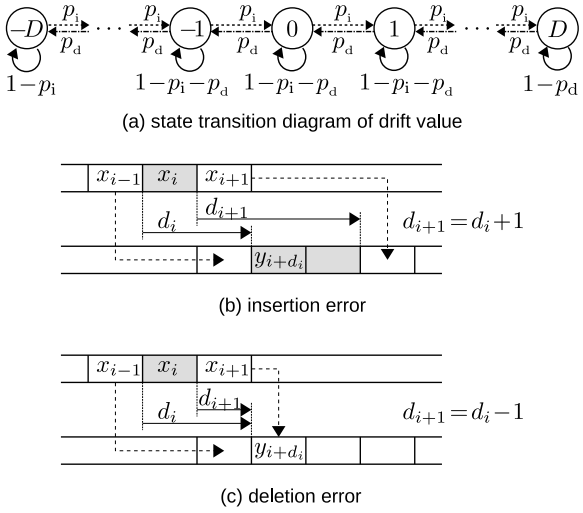

Fig. 1 Channel model.

$$|\mathcal{I}(i; d_i, d_{i+1})| = \begin{cases} 2 & (d_{i+1} = d_i + 1 \text{ (insertion)}) \\ 1 & (d_{i+1} = d_i) \\ 0 & (d_{i+1} = d_i - 1 \text{ (deletion)}) \end{cases},$$

$$\forall i, j \in \mathbb{Z}_N, (i \ne j) \rightarrow \mathcal{I}(i; d_i, d_{i+1}) \cap \mathcal{I}(j; d_j, d_{j+1}) = \phi,$$

$$\bigcup_{i \in \mathbb{Z}_N} \mathcal{I}(i; d_i, d_{i+1}) = \mathbb{Z}_{N'},$$

where ϕ is the empty set. For each transmitted bit x_i ($i \in \mathbb{Z}_N$), received bit values are determined according to

$$p(y_{i'}|x_i) = \begin{cases} 1 - p_\text{s} & (y_{i'} = x_i) \\ p_\text{s} & (y_{i'} = \overline{x}_i) \end{cases},$$

where $i' \in \mathcal{I}(i; d_i, d_{i+1})$. Figure 1 (b) and (c) illustrate the relations between drift value d_i and insertion/deletion error.

4. Polar Code for IDS Channel

Let $N = 2^n$ be the code length of polar code. Let $\mathcal{A}$ and $\mathcal{A}^c$ be sets of information and frozen bits, respectively, where $\mathcal{A} \cup \mathcal{A}^c = \mathbb{Z}_N$ and $\mathcal{A} \cap \mathcal{A}^c = \phi$. The positions of frozen bits are determined based on a simulation based estimation described in Sect. 4.3. It is assumed that the value of frozen bit is zero, while effect of frozen bit values on the decoded error rate will be examined by simulation in Sect. 5.2. Encoding and decoding use $n + 1$ intermediate binary vectors, $\boldsymbol{u}(n)$, $\boldsymbol{u}(n-1), \ldots, \boldsymbol{u}(0) \in \mathbb{B}^N$, each of length $N = 2^n$. Figure 2 illustrates notations in the encoding and decoding procedures.

4.1 Encoding

Encoding process is identical to that of the original polar code. That is, information word $\boldsymbol{u}_0^{N-1} = \boldsymbol{u}(n)$ is encoded as $\boldsymbol{x}_0^{N-1} = \boldsymbol{u}(0)$ by the following recursive calculation:

$$\boldsymbol{u}(n) = \boldsymbol{u}_0^{N-1},$$

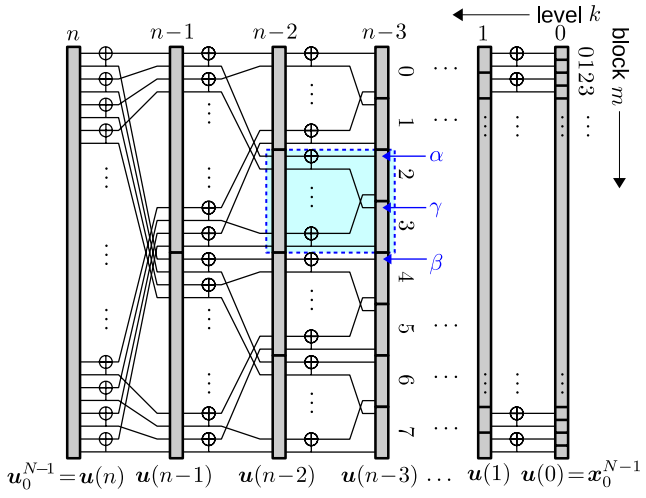

Fig. 2 Notations for encoding and decoding.

$$\begin{aligned}
\boldsymbol{u}(k-1)_{\alpha}^{\gamma-1} &= \mathrm{even}\left(\boldsymbol{u}(k)_{\alpha}^{\beta-1}\right) \oplus \mathrm{odd}\left(\boldsymbol{u}(k)_{\alpha}^{\beta-1}\right),\\
\boldsymbol{u}(k-1)_{\gamma}^{\beta-1} &= \mathrm{odd}\left(\boldsymbol{u}(k)_{\alpha}^{\beta-1}\right),\\
\boldsymbol{x}_0^{N-1} &= \boldsymbol{u}(0),
\end{aligned}$$

where $k \in \{1, 2, \ldots, n\}$ is *level* index, and α, β, and γ are bit positions given as

$$\begin{aligned}
&\alpha = 2^k m, \quad \beta = 2^k(m+1),\\
&\gamma = (\alpha+\beta)/2 = 2^k m + 2^{k-1}.
\end{aligned}$$

Here, $m \in \{0, 1, \ldots, 2^{n-k}-1\}$ indicates *block* index.

4.2 Successive Cancellation Decoding

The SC decoder is given the frozen bit set $\mathcal{A}^c \subset \mathbb{Z}_N$, value of each frozen bit, and channel parameters, $p_\mathrm{i}, p_\mathrm{d}, p_\mathrm{s}$, and D. The decoder inputs received word $\boldsymbol{y}_0^{N'-1} \in \mathbb{B}^{N'}$ with its length N', and it outputs decoded word $\hat{\boldsymbol{u}}_0^{N-1} = (\hat{u}_0, \hat{u}_1, \ldots, \hat{u}_{N-1}) \in \mathbb{B}^N$. The original SC decoding is modified to deal with drift d_i, as follows.

The i-th information bit u_i is estimated as

$$\hat{u}_i = \begin{cases} u_i & (i \in \mathcal{A}^c)\\ h_i\left(N', \boldsymbol{y}_0^{N'-1}, \hat{\boldsymbol{u}}_0^{i-1}\right) & (i \in \mathcal{A}) \end{cases},$$

where

$$\begin{aligned}
&h_i\left(N', \boldsymbol{y}_0^{N'-1}, \hat{\boldsymbol{u}}_0^{i-1}\right)\\
&= \begin{cases} 0 & \left(\frac{p\left(d_N, \boldsymbol{y}_0^{N'-1}, \boldsymbol{u}_0^{i-1}=\hat{\boldsymbol{u}}_0^{i-1} \mid u_i=0\right)}{p\left(d_N, \boldsymbol{y}_0^{N'-1}, \boldsymbol{u}_0^{i-1}=\hat{\boldsymbol{u}}_0^{i-1} \mid u_i=1\right)} \geq 1\right)\\ 1 & (\text{otherwise}) \end{cases}.
\end{aligned}$$

We firstly consider a polar bit IDS channel of level $k = n$ for $\boldsymbol{u}(n) = \boldsymbol{u}_0^{N-1}$ defined as follows:

$$\begin{aligned}
&W_{2^n}^{(i)}\left(d_N, \boldsymbol{y}_0^{N'-1}, \boldsymbol{u}(n)_0^{i-1} = \hat{\boldsymbol{u}}_0^{i-1} \middle| d_0 = 0, \boldsymbol{u}(n)_i = c\right)\\
&\quad = p\left(d_N, \boldsymbol{y}_0^{N'-1}, \boldsymbol{u}_0^{i-1} = \hat{\boldsymbol{u}}_0^{i-1} \middle| d_0 = 0, u_i = c\right),
\end{aligned}$$

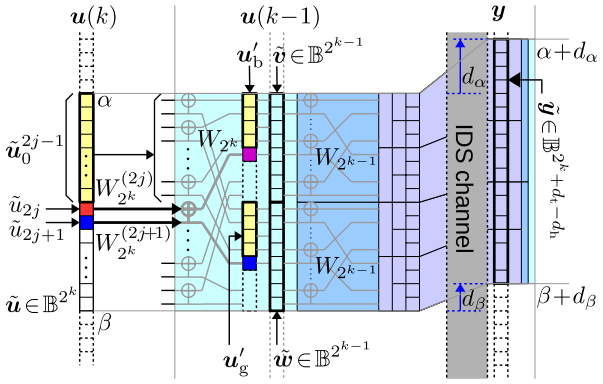

Fig. 3 Polar bit IDS channel of level k.

where $c \in \mathbb{B}$. This channel is factorized into two channels of $W_{2^{n-1}}^{(\lfloor i/2 \rfloor)}(\cdot)$ in level $k = n-1$. Similarly, we can apply recursive factorization of the polar bit IDS channel in level k, $W_{2^k}^{(i)}(\cdot)$, into two channels in level $k-1$, $W_{2^{k-1}}^{(\lfloor i/2 \rfloor)}(\cdot)$. Unlike the existing SC decoding, the following SC decoding considers cases in which sub-vector of received word $\boldsymbol{y}$ is factorized into two vectors of unequal lengths due to insertion and deletion errors. Figure 3 illustrates the polar bit IDS channel corresponding to level k.

4.2.1 Recursions for Level $k \in \{1, 2, \ldots, n\}$

Probabilities in level k are calculated using probabilities in level $k-1$. In level k, probability is calculated for each combination (m, j) of block index $m \in \{0, 1, \ldots, 2^{n-k}-1\}$ and bit index $j \in \{0, 1, \ldots, 2^{k-1}-1\}$. The following notations are used in the recursion:

$$\begin{aligned}
&\alpha = 2^k m,\ \beta = 2^k(m+1),\ \gamma = (\alpha+\beta)/2,\\
&\tilde{\boldsymbol{u}} = (\tilde{u}_0, \tilde{u}_1, \ldots, \tilde{u}_{2^k-1}) = \boldsymbol{u}(k)_{\alpha}^{\beta-1} \in \mathbb{B}^{2^k},\\
&\tilde{\boldsymbol{v}} = (\tilde{v}_0, \tilde{v}_1, \ldots, \tilde{v}_{2^{k-1}-1}) = \boldsymbol{u}(k-1)_{\alpha}^{\gamma-1} \in \mathbb{B}^{2^{k-1}},\\
&\tilde{\boldsymbol{w}} = (\tilde{w}_0, \tilde{w}_1, \ldots, \tilde{w}_{2^{k-1}-1}) = \boldsymbol{u}(k-1)_{\gamma}^{\beta-1} \in \mathbb{B}^{2^{k-1}},\\
&\boldsymbol{u}'_\mathrm{b} = \mathrm{even}\left(\tilde{\boldsymbol{u}}_0^{2j-1}\right) \oplus \mathrm{odd}\left(\tilde{\boldsymbol{u}}_0^{2j-1}\right) \in \mathbb{B}^j,\\
&\boldsymbol{u}'_\mathrm{g} = \mathrm{odd}\left(\tilde{\boldsymbol{u}}_0^{2j-1}\right) \in \mathbb{B}^j.
\end{aligned}$$

The probabilities for bits of even indices are calculated as follows:

$$\begin{aligned}
&W_{2^k}^{(2j)}\left(d_\beta, \boldsymbol{y}_{\alpha+d_\alpha}^{\beta+d_\beta-1}, \tilde{\boldsymbol{u}}_0^{2j-1} \middle| d_\alpha, \tilde{u}_{2j}\right)\\
&= \sum_{\tilde{u}_{2j+1} \in \mathbb{B}} p\left(d_\beta, \boldsymbol{y}_{\alpha+d_\alpha}^{\beta+d_\beta-1}, \tilde{\boldsymbol{u}}_0^{2j-1}, \tilde{u}_{2j+1} \middle| d_\alpha, \tilde{u}_{2j}\right)\\
&= \sum_{\tilde{u}_{2j+1} \in \mathbb{B}} p\left(d_\beta, \boldsymbol{y}_{\alpha+d_\alpha}^{\beta+d_\beta-1}, \tilde{\boldsymbol{u}}_0^{2j-1} \middle| d_\alpha, \tilde{u}_{2j}, \tilde{u}_{2j+1}\right) p\left(\tilde{u}_{2j+1} \middle| \tilde{u}_{2j}\right)\\
&= \sum_{\tilde{u}_{2j+1} \in \mathbb{B}} p\left(d_\beta, \boldsymbol{y}_{\alpha+d_\alpha}^{\beta+d_\beta-1}, \tilde{\boldsymbol{v}}_0^{j-1} = \boldsymbol{u}'_\mathrm{b}, \tilde{\boldsymbol{w}}_0^{j-1} = \boldsymbol{u}'_\mathrm{g}\right.\\
&\qquad \left. \middle| d_\alpha, \tilde{v}_j = \tilde{u}_{2j} \oplus \tilde{u}_{2j+1}, \tilde{w}_j = \tilde{u}_{2j+1}\right) \cdot \frac{1}{2}\\
&= \frac{1}{2} \sum_{d_\gamma \in \mathcal{D}} \sum_{\tilde{u}_{2j+1} \in \mathbb{B}} p\left(d_\beta, d_\gamma, \boldsymbol{y}_{\alpha+d_\alpha}^{\gamma+d_\gamma-1}, \boldsymbol{y}_{\gamma+d_\gamma}^{\beta+d_\beta-1}, \tilde{\boldsymbol{v}}_0^{j-1} = \boldsymbol{u}'_\mathrm{b}, \tilde{\boldsymbol{w}}_0^{j-1} = \boldsymbol{u}'_\mathrm{g}\right.
\end{aligned}$$

$$\left| d_\alpha, \tilde{v}_j = \tilde{u}_{2j} \oplus \tilde{u}_{2j+1}, \tilde{w}_j = \tilde{u}_{2j+1} \right)$$
$$= \frac{1}{2} \sum_{d_\gamma \in \mathcal{D}} \sum_{\tilde{u}_{2j+1} \in \mathbb{B}} W_{2^{k-1}}^{(j)} \left(d_\gamma, \boldsymbol{y}_{\alpha+d_\alpha}^{\gamma+d_\gamma-1}, \tilde{\boldsymbol{v}}_0^{j-1} = \boldsymbol{u}'_{\mathrm{b}} \middle| d_\alpha, \tilde{v}_j = \tilde{u}_{2j} \oplus \tilde{u}_{2j+1} \right)$$
$$\times W_{2^{k-1}}^{(j)} \left(d_\beta, \boldsymbol{y}_{\gamma+d_\gamma}^{\beta+d_\beta-1}, \tilde{\boldsymbol{w}}_0^{j-1} = \boldsymbol{u}'_{\mathrm{g}} \middle| d_\gamma, \tilde{w}_j = \tilde{u}_{2j+1} \right),$$

Those of odd indices are calculated as follows:

$$W_{2^k}^{(2j+1)} \left(d_\beta, \boldsymbol{y}_{\alpha+d_\alpha}^{\beta+d_\beta-1}, \tilde{\boldsymbol{u}}_0^{2j} \middle| d_\alpha, \tilde{u}_{2j+1} \right)$$
$$= p \left(d_\beta, \boldsymbol{y}_{\alpha+d_\alpha}^{\beta+d_\beta-1}, \tilde{\boldsymbol{u}}_0^{2j-1} \middle| d_\alpha, \tilde{u}_{2j}, \tilde{u}_{2j+1} \right) p \left(\tilde{u}_{2j} \middle| \tilde{u}_{2j+1} \right)$$
$$= p \left(d_\beta, \boldsymbol{y}_{\alpha+d_\alpha}^{\beta+d_\beta-1}, \tilde{\boldsymbol{v}}_0^{j-1} = \boldsymbol{u}'_{\mathrm{b}}, \tilde{\boldsymbol{w}}_0^{j-1} = \boldsymbol{u}'_{\mathrm{g}} \right.$$
$$\left. \middle| d_\alpha, \tilde{v}_j = \tilde{u}_{2j} \oplus \tilde{u}_{2j+1}, \tilde{w}_j = \tilde{u}_{2j+1} \right) \cdot \frac{1}{2}$$
$$= \frac{1}{2} \sum_{d_\gamma \in \mathcal{D}} p \left(d_\beta, d_\gamma, \boldsymbol{y}_{\alpha+d_\alpha}^{\gamma+d_\gamma-1}, \boldsymbol{y}_{\gamma+d_\gamma}^{\beta+d_\beta-1}, \tilde{\boldsymbol{v}}_0^{j-1} = \boldsymbol{u}'_{\mathrm{b}}, \tilde{\boldsymbol{w}}_0^{j-1} = \boldsymbol{u}'_{\mathrm{g}} \right.$$
$$\left. \middle| d_\alpha, \tilde{v}_j = \tilde{u}_{2j} \oplus \tilde{u}_{2j+1}, \tilde{w}_j = \tilde{u}_{2j+1} \right)$$
$$= \frac{1}{2} \sum_{d_\gamma \in \mathcal{D}} W_{2^{k-1}}^{(j)} \left(d_\gamma, \boldsymbol{y}_{\alpha+d_\alpha}^{\gamma+d_\gamma-1}, \tilde{\boldsymbol{v}}_0^{j-1} = \boldsymbol{u}'_{\mathrm{b}} \middle| d_\alpha, \tilde{v}_j = \tilde{u}_{2j} \oplus \tilde{u}_{2j+1} \right)$$
$$\times W_{2^{k-1}}^{(j)} \left(d_\beta, \boldsymbol{y}_{\gamma+d_\gamma}^{\beta+d_\beta-1}, \tilde{\boldsymbol{w}}_0^{j-1} = \boldsymbol{u}'_{\mathrm{g}} \middle| d_\gamma, \tilde{w}_j = \tilde{u}_{2j+1} \right).$$

The above calculations assume that the following relation holds:

$$p \left(\tilde{u}_{2j+1} \middle| \tilde{u}_{2j} \right) = p \left(\tilde{u}_{2j} \middle| \tilde{u}_{2j+1} \right) = 1/2.$$

4.2.2 Calculation for Level $k = 0$

For $i \in \{0, 1, \ldots, N-1\}$, the probability is calculated as

$$W_{2^0}^{(i)} \left(d_{i+1}, \boldsymbol{y}_{i+d_i}^{(i+1)+d_{i+1}-1} \middle| d_i, \boldsymbol{u}(0)_i \right)$$
$$= p \left(\boldsymbol{y}_{i+d_i}^{i+d_{i+1}} \middle| d_i, d_{i+1}, x_i \right) \cdot p(d_{i+1} | d_i).$$

Here, the second factor of right-hand side is given by Eq. (1), and the first factor is calculated as

$$p \left(\boldsymbol{y}_{i+d_i}^{i+d_{i+1}} \middle| d_i, d_{i+1}, x_i \right) =$$
$$\begin{cases} p_{\mathrm{s}}^{\delta} (1-p_{\mathrm{s}})^{\ell-\delta} & (|d_{i+1} - d_i| \le 1, 0 \le i + d_i, i + d_{i+1} < N') \\ 0 & (\text{otherwise}) \end{cases},$$

where $\ell = |\mathcal{I}(i; d_i, d_{i+1})|$ and

$$\delta = \left| \{ i' \in \mathcal{I}(i; d_i, d_{i+1}) \mid y_{i'} \neq x_i \} \right|$$
$$= \sum_{i' \in \mathcal{I}(i; d_i, d_{i+1})} (x_i \oplus y_{i'}).$$

This SC decoding can be extended to the list decoding in the same way as the existing SCL decoding [13], and also concatenation with a CRC is straightforward.

4.3 Determination of Frozen Bits

Let $I(W_N^{(i)})$ be the symmetric capacity of $W_N^{(i)}$ defined as

$$I \left(W_N^{(i)} \right) =$$
$$\frac{1}{2^N} \sum_{\boldsymbol{u} \in \mathbb{B}^N} \sum_{\boldsymbol{y} \in \mathcal{B}} p \left(\boldsymbol{y}_0^{N'-1} \middle| \boldsymbol{u}_0^{N-1} \right) \tilde{I} \left(d_N, \boldsymbol{y}_0^{N'-1}, \boldsymbol{u}_0^{i-1} \middle| u_i \right), \quad (2)$$

where $\mathcal{B} = \bigcup_{d \in \mathcal{D}} \mathbb{B}^{N+d}$ and

$$\tilde{I} \left(d_N, \boldsymbol{y}_0^{N'-1}, \boldsymbol{u}_0^{i-1} \middle| u_i \right) =$$
$$\log \frac{p \left(d_N, \boldsymbol{y}_0^{N'-1}, \boldsymbol{u}_0^{i-1} \middle| u_i \right)}{\frac{1}{2} p \left(d_N, \boldsymbol{y}_0^{N'-1}, \boldsymbol{u}_0^{i-1} \middle| u_i \right) + \frac{1}{2} p \left(d_N, \boldsymbol{y}_0^{N'-1}, \boldsymbol{u}_0^{i-1} \middle| \bar{u}_i \right)}. \quad (3)$$

For given code length N and rate R, the set of positions of frozen bits is determined as

$$\mathcal{A}^c = \{ i_0, i_1, \ldots, i_{m-1} \} \subset \mathbb{Z}_N,$$

where $m = [NR]$ is the round-off of NR, and

$$\forall i, j \in \mathbb{Z}_N, (i \in \mathcal{A}^c \wedge j \in \mathcal{A}) \to I \left(W_N^{(i)} \right) \le I \left(W_N^{(j)} \right).$$

For the polar bit IDS channel, it will be difficult to calculate the exact value of the symmetric capacity $I(W_N^{(i)})$. Observing that Eq. (2) is the expectation of Eq. (3) over all received words $\boldsymbol{y}_0^{N'-1}$ for a given codeword $\boldsymbol{u}_0^{N-1}$, where $\boldsymbol{u}$ is uniformly distributed, we use the following simulation based method to estimate the symmetric capacity.

1. Generate a random information vector $\boldsymbol{u}_0^{N-1}$.
2. Encode $\boldsymbol{u}_0^{N-1}$ to codeword $\boldsymbol{x}_0^{N-1}$.
3. Determine received word $\boldsymbol{y}_0^{N'-1}$ probabilistically according to the IDS channel model.
4. Calculate $\lambda = \tilde{I} \left(d_N, \boldsymbol{y}_0^{N'-1}, \boldsymbol{u}_0^{i-1} \middle| u_i \right)$ of Eq. (3) using the modified SC decoding.
5. Repeat the above procedure for a fixed number of times, and then determine the average of λ as the symmetric capacity.

4.4 Estimation of Block Error Rate

For given $\mathcal{A} = \mathbb{Z}_N \setminus \mathcal{A}^c$, an upper bound on decoded block error rate (BLER) of the above SC decoding is derived as follows [11]:

$$p(\mathcal{E}) \le \sum_{i \in \mathcal{A}} p(\mathcal{E}_i), \quad (4)$$

where $\mathcal{E}_i$ is the event that the i-th bit is incorrectly decoded as $\hat{u}_i = \bar{u}_i$, $\mathcal{E}$ is the event that a decoded word has at least one incorrectly decoded bit, and

$$p(\mathcal{E}_i) =$$
$$\frac{1}{2^N} \sum_{\boldsymbol{u} \in \mathbb{B}^N} \sum_{\boldsymbol{y} \in \mathcal{B}} p \left(\boldsymbol{y}_0^{N'-1} \middle| \boldsymbol{u}_0^{N-1} \right) F_i \left(d_N, \boldsymbol{y}_0^{N'-1}, \boldsymbol{u}_0^{i-1} \middle| u_i \right). \quad (5)$$

Here, $F_i(\cdot) \in \mathbb{B}$ is defined using the indicator function $\mathbb{1}$ as

$$F_i \left(d_N, \boldsymbol{y}_0^{N'-1}, \boldsymbol{u}_0^{i-1} \middle| u_i \right) =$$

$$\begin{cases} \mathbb{1}\left(p\left(d_N, \boldsymbol{y}_0^{N'-1}, \boldsymbol{u}_0^{i-1} \middle| 0\right) < p\left(d_N, \boldsymbol{y}_0^{N'-1}, \boldsymbol{u}_0^{i-1} \middle| 1\right)\right) & (u_i = 0) \\ \mathbb{1}\left(p\left(d_N, \boldsymbol{y}_0^{N'-1}, \boldsymbol{u}_0^{i-1} \middle| 1\right) \le p\left(d_N, \boldsymbol{y}_0^{N'-1}, \boldsymbol{u}_0^{i-1} \middle| 0\right)\right) & (u_i = 1) \end{cases}. \tag{6}$$

Similar to the estimation of symmetric capacity based on Eqs. (2) and (3), the value of $p(\mathcal{E}_i)$ is estimated by a simulation based method since Eq. (5) is the expectation of Eq. (6) over all received words $\boldsymbol{y}_0^{N'-1}$ for a given codeword $\boldsymbol{u}_0^{N-1}$, where $\boldsymbol{u}$ is uniformly distributed. Numerical example of the estimated BLER will be shown in Fig. 8 of Sect. 5.2.

4.5 Computational Complexity

Recursion structure of the original SC decoding is expressed as follows:

$$W_{2^k}^{(2j)}(\cdot|\tilde{u}_{2j}) = \frac{1}{2}\sum_{\tilde{u}_{2j+1}\in\mathbb{B}} W_{2^{k-1}}^{(j)}(\cdot|\tilde{u}_{2j}\oplus\tilde{u}_{2j+1}) W_{2^{k-1}}^{(j)}(\cdot|\tilde{u}_{2j+1}),$$

$$W_{2^k}^{(2j+1)}(\cdot|\tilde{u}_{2j+1}) = \frac{1}{2} W_{2^{k-1}}^{(j)}(\cdot|\tilde{u}_{2j}\oplus\tilde{u}_{2j+1}) W_{2^{k-1}}^{(j)}(\cdot|\tilde{u}_{2j+1}),$$

where $\tilde{\boldsymbol{u}} = (\tilde{u}_0, \tilde{u}_1, \ldots, \tilde{u}_{N-1}) = \boldsymbol{u}(k)$. The probability is calculated for each element $\tilde{u}_i$ of each intermediate vector $\boldsymbol{u}(k)$, where $i \in \mathbb{Z}_N$ and $k \in \mathbb{Z}_n$. Hence computational complexity is $O(N \log N)$. On the other hand, recursion of the presented SC decoding for IDS channel is expressed as follows:

$$W_{2^k}^{(2j)}(d_\beta, \cdot\,|d_\alpha, \tilde{u}_{2j}) =$$
$$\frac{1}{2}\sum_{d_\gamma\in\mathcal{D}}\sum_{\tilde{u}_{2j+1}\in\mathbb{B}} W_{2^{k-1}}^{(j)}(d_\gamma, \cdot\,|d_\alpha, \tilde{u}_{2j}\oplus\tilde{u}_{2j+1}) W_{2^{k-1}}^{(j)}(d_\beta, \cdot\,|d_\gamma, \tilde{u}_{2j+1}),$$

$$W_{2^k}^{(2j+1)}(d_\beta, \cdot\,|d_\alpha, \tilde{u}_{2j+1}) =$$
$$\frac{1}{2}\sum_{d_\gamma\in\mathcal{D}} W_{2^{k-1}}^{(j)}(d_\gamma, \cdot\,|d_\alpha, \tilde{u}_{2j}\oplus\tilde{u}_{2j+1}) W_{2^{k-1}}^{(j)}(d_\beta, \cdot\,|d_\gamma, \tilde{u}_{2j+1}),$$

where $d_\alpha, d_\beta \in \mathcal{D}$. From the above relations, the number of calculated probabilities is increased by a factor of $|\mathcal{D}|^2 = (2D+1)^2$, and the complexity of calculation of each probability is increased by a factor of $|\mathcal{D}| = 2D+1$. Thus, the complexity of the presented SC decoding is $O(D^3)$ with respect to the maximum drift value D, while it is still $O(N \log N)$ with respect to the code length N.

5. Simulation Results

Numerical results of polarization of $W_{2^n}^{(i)}$ and decoded error rates are presented in Sects. 5.1 and 5.2, respectively. We assume that the maximum drift values is $D = 4$ in the following simulations.

5.1 Channel Polarization

Figure 4 presents relation between the bit index i of $W_{2^n}^{(i)}$ and symmetric capacity $I(W_{2^n}^{(i)})$ estimated by the simulation described in Sect. 4.3, where $p_\mathrm{i} = p_\mathrm{d} = 1.0 \times 10^{-2}$, $p_\mathrm{s} = 1.0 \times 10^{-2}$, and $n = 12$. This simulation result suggests polarization of $W_{2^n}^{(i)}$ similar to memoryless channels. For $p_\mathrm{i} = p_\mathrm{d} = 5.0 \times 10^{-3}$ and $p_\mathrm{s} = 0$, Fig. 5 shows the relation

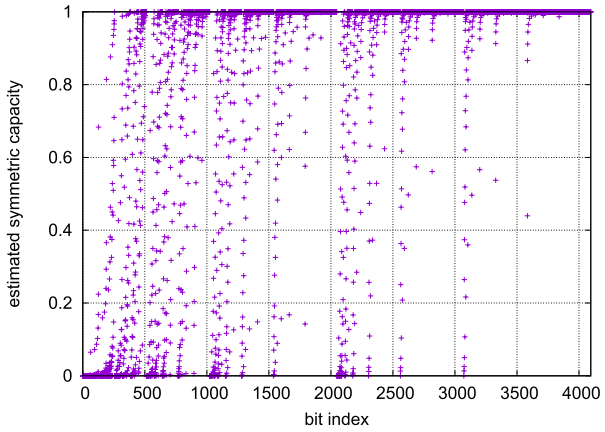

Fig. 4 Polarization of IDS channel ($p_\mathrm{i} = p_\mathrm{d} = 1.0 \times 10^{-2}$, $p_\mathrm{s} = 1.0 \times 10^{-2}$, $n = 12$).

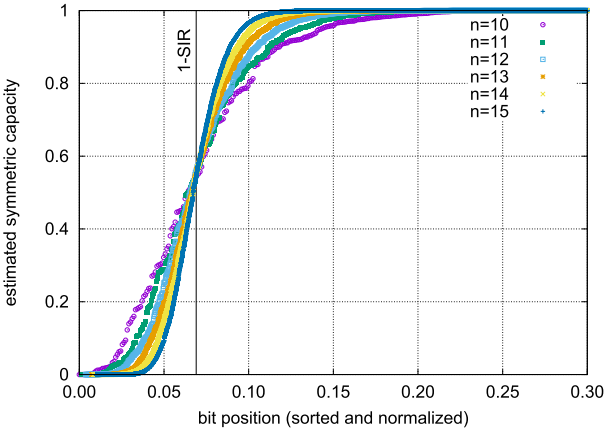

Fig. 5 Relation between bit position and mutual information ($p_\mathrm{i} = p_\mathrm{d} = 5.0 \times 10^{-3}$, $p_\mathrm{s} = 0$, SIR $= 9.31 \times 10^{-1}$).

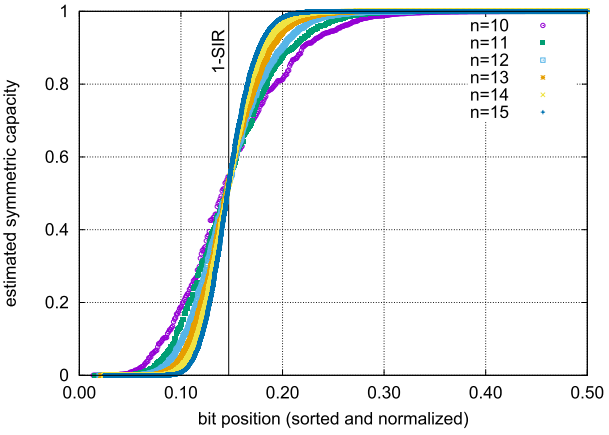

Fig. 6 Relation between bit position and mutual information ($p_\mathrm{i} = p_\mathrm{d} = 5.0 \times 10^{-3}$, $p_\mathrm{s} = 1.0 \times 10^{-2}$, SIR $= 8.53 \times 10^{-1}$).

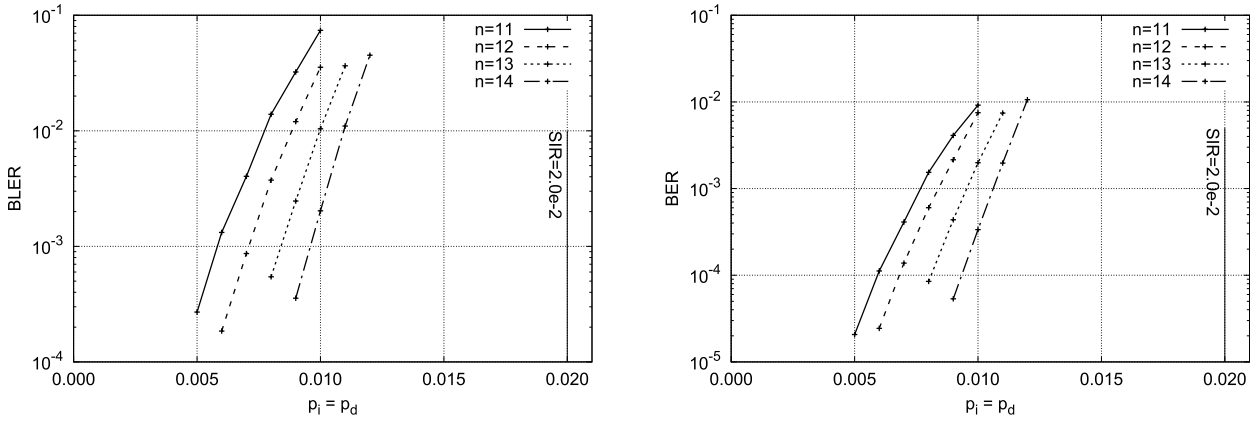

Fig. 7 Dependence of error rates on the code length $N = 2^n$ ($n \in \{11, 12, 13, 14\}$, $p_s = 0$, $R = 0.80$, $L = 4$).

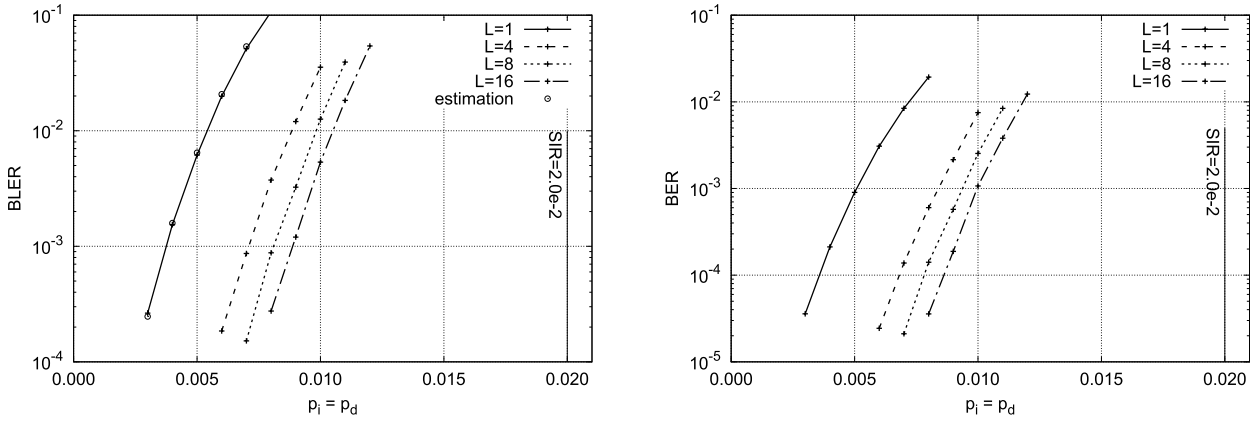

Fig. 8 Dependence of error rates on the list size $L \in \{1, 4, 8, 16\}$ ($p_s = 0$, $n = 12$, $R = 0.80$).

between bit position (sorted by $I(W_{2^n}^{(i)})$ and normalized by code length $N = 2^n$) and estimated symmetric capacity, where $n \in \{10, 11, \ldots, 15\}$. The result suggests that longer codes have stronger polarization effect, and it is expected that the rate $\left|\left\{i \in \mathbb{Z}_N \;\middle|\; I(W_{2^n}^{(i)}) > 1 - \epsilon\right\}\right| / N$ approaches the channel SIR, 9.31×10^{-1}. Figure 6 presents the case of channel with substitution errors, where $p_s = 1.0 \times 10^{-2}$. This channel also shows the polarization effect similar to Fig. 5.

5.2 Block and Bit Error Rates

The block error rate (BLER) and bit error rate (BER) of the presented coding are evaluated by simulations, where the positions of frozen bits are determined according to the procedure of Sect. 4.3 with 10^4 iterations. The value of frozen bit is $u_i = 0$ for all $i \in \mathcal{A}^c$, except in Paragraph (6) wherein the effect of frozen bit values on decoded error rate is examined. The CRC for SCL decoding is defined by generator polynomial $g(x) = x^8 + x^7 + x^6 + x^4 + x^2 + 1$.

(1) Relation to the Code Length $N = 2^n$

Figure 7 shows the BLER and BER for code lengths $N = 2^n$, where $n \in \{11, 12, 13, 14\}$. Here, the horizontal axis is the insertion/deletion probability $p_i = p_s$, the substitution probability is $p_s = 0$, code rate $R = 0.80$, and list size $L = 4$. It is observed that the error rate lowers with increasing code length, while at these code lengths, there exists considerable gap from the channel SIR.

(2) Relation to the List Size L

Figure 8 presents effect of the list size $L \in \{1, 4, 8, 16\}$ on the decoded BLER and BER, where the code length is $N = 2^{12}$ and code rate is $R = 0.80$. The results show that the SCL decoding has much lower error rate compared to the SC decoding ($L = 1$), while the improvement diminishes for larger list sizes. This figure also shows the estimated BLER of SC decoding ($L = 1$) given by the right-hand side of Eq. (4). The estimation gives accurate values of BLER for the simulated parameters.

(3) Comparison to Marker-Based Codings

Figure 9 compares the error rates of the polar codes with those of marker-based coding [9], where $p_s = 0, n \in \{12, 13\}$, $R = 0.80$, and $L = 16$. The outer code of the marker-based coding is binary (3,6)-regular LDPC code of rate 0.88, and the inner code is insertion of marker $(0, 1)$ with the regular interval of 20 bits. The results show that the error rates

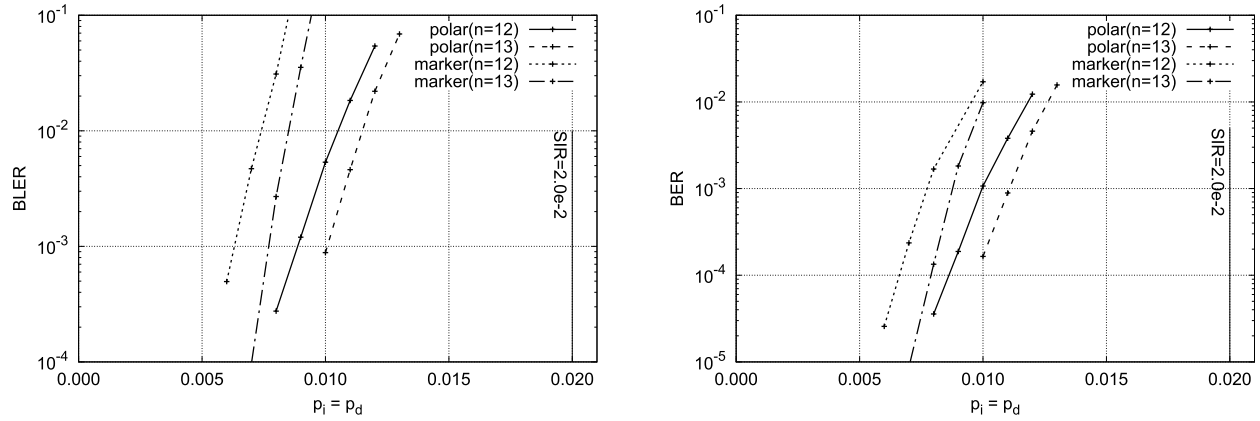

Fig. 9 Comparison to marker-based codings ($p_s = 0$, $n \in \{12, 13\}$, $R = 0.80$, $L = 16$).

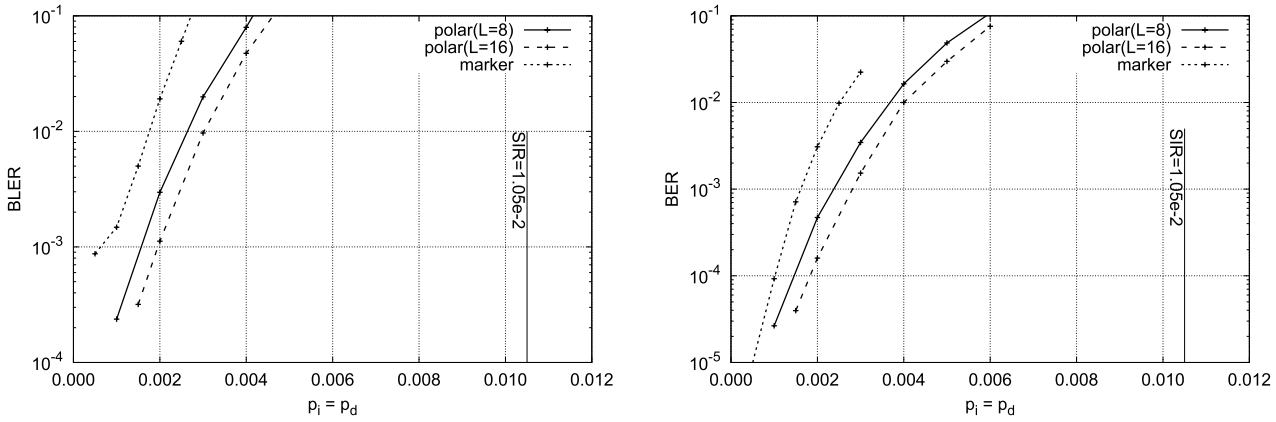

Fig. 10 Error rate when channel has substitution errors ($p_s = 1.0\times10^{-2}$, $n = 12$, $R = 0.80$, $L \in \{8, 16\}$).

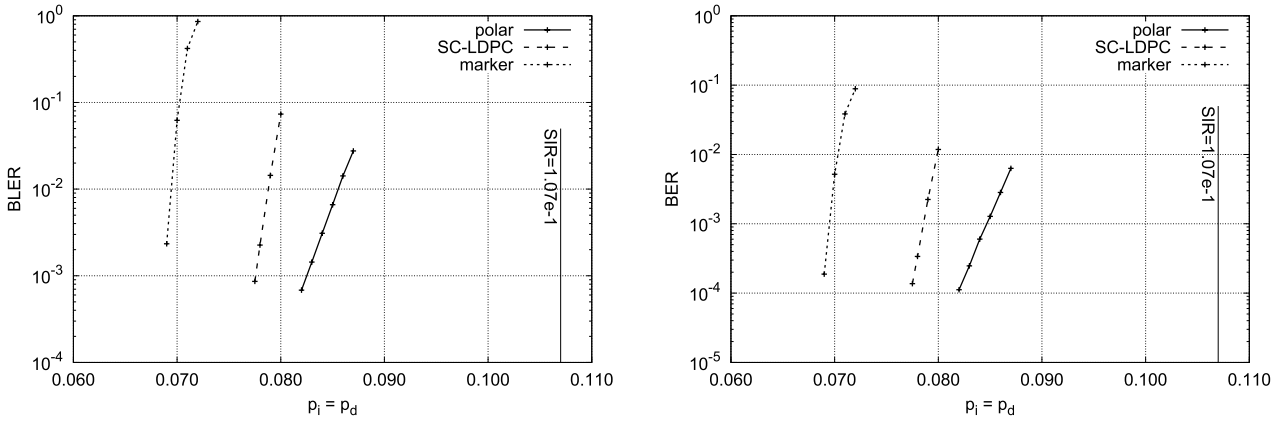

Fig. 11 Error rates of low-rate codes ($p_s = 0$, $n = 17$, $R = 0.44$, $L = 8$).

of polar code are lower than those of marker-based codings.

(4) Error Rates of Channels with Substitution Errors

Figure 10 presents the error rates of polar code and marker-based coding when the substitution error probability is $p_s = 1.0\times10^{-2}$, where the marker coding is with the interval of 96 bits. The polar codes have lower error rates compared to the marker-based coding, while discrepancy from the SIR ($= 1.05\times10^{-2}$) is large. For small insertion/deletion probabilities, e.g., $p_i = p_d = 1.0\times10^{-3}$, substitution errors with probability $p_s = 2.0\times10^{-2}$ have a dominant contribution to the decoded error rates, and hence error rates do not fall sharply.

(5) Error Rates of Low-Rate Codes with Large Length

Figure 11 shows the error rates of low-rate codes with $R =$

Table 1 Effect of frozen bit values on decoded error rate ($p_s = 0, n = 12, R = 0.80, L = 16$).

	BLER			BER		
$p_i = p_d$	(a)	(b)	(c)	(a)	(b)	(c)
0.009	1.3×10^{-3}	1.2×10^{-3}	1.3×10^{-3}	2.1×10^{-4}	2.0×10^{-4}	1.9×10^{-4}
0.010	5.2×10^{-3}	5.1×10^{-3}	5.1×10^{-3}	9.3×10^{-4}	9.2×10^{-4}	9.2×10^{-4}
0.011	1.7×10^{-2}	1.9×10^{-2}	1.7×10^{-2}	3.4×10^{-3}	3.8×10^{-3}	3.4×10^{-3}
0.012	5.2×10^{-2}	5.1×10^{-2}	5.1×10^{-2}	1.1×10^{-2}	1.1×10^{-2}	1.1×10^{-2}

0.44, $n = 17$, and $p_s = 0$. This figure shows the BLERs and BERs of the polar code, marker-based coding, and spatially-coupled LDPC (SC-LDPC) code [10]. The outer code of the marker-based coding is binary (3,6)-regular LDPC code of rate 0.58, and the inner code is insertion of marker (0, 1) with the interval of 6 bits. The base matrix of SC-LDPC code is $B(3, 6, 16)$ and the lifting number is $M = 4096$. The results show that polar code has the lowest error rate among the evaluated codes.

(6) Effect of Frozen Bit Values

Table 1 lists the error rates for three cases of frozen bit values, where the values are determined as (a) $u_i = 0$, (b) $u_i = 1$, and (c) $u_i \in \mathbb{B}$ with $p(u_i = 0) = p(u_i = 1) = 1/2$, for $i \in \mathcal{A}^c$. Here, the channel and code parameters are determined as $p_s = 0, n = 12, R = 0.80$, and $L = 16$. The results do not show significant dependence of error rates on the frozen bit values, and thus it is expected that the IDS channel is symmetric with respect to input bit value.

6. Conclusion

This paper presented an SC decoding of polar codes modified for IDS error channels, in which insertions and deletions are expressed by drift values. The recursive computations of original SC decoding is modified to include drift values in the calculation. The computational complexity of the SC decoding is $O(D^3)$ with respect to the maximum drift value D, and $O(N \log N)$ with respect to the code length N. This also showed a simulation based estimation of symmetric capacity of polar bit channels to determine the positions of frozen bits. Simulation results showed that the presented SC list decoding with CRC gives lower decoded error rates compared to the existing codes, such as spatially-coupled code, and concatenated coding with LDPC code and synchronization marker. Future works include reduction of decoding complexity by approximation, theoretical analysis and proof of polarization of polar bit IDS channel, theoretical analysis on the decoded error rate of the modified SC list decoding, and efficient determination method of frozen bits.

Acknowledgments

This work was supported by JSPS KAKENHI 18K04125.

References

[1] S. Zhang, K.S. Chai, K. Cai, B. Chen, Z. Qin, and S.M. Foo, "Write failure analysis for bit-patterned-media recording and its impact on read channel modeling," IEEE Trans. Magn., vol.46, no.6, pp.1363–1365, 2010.
[2] Y.M. Chee, H.M. Kiah, A. Vardy, V.K. Vu, and E. Yaakobi, "Coding for racetrack memories," Proc. 2017 IEEE Int. Symp. Information Theory, pp.619–623, 2017.
[3] R. Shibata, G. Hosoya, and H. Yashima, "Joint iterative decoding of spatially coupled low-density parity-check codes for position errors in racetrack memories," IEICE Trans. Fundamentals, vol.E101-A, no.12, pp.2055–2063, Dec. 2018.
[4] W. Mao, S.N. Diggavi, and S. Kannan, "Models and information-theoretic bounds for nanopore sequencing," IEEE Trans. Inf. Theory, vol.64, no.4, pp.3216–3236, 2018.
[5] V.I. Levenshtein, "Binary codes capable of correcting deletions, insertions, and reversals," Soviet physics doklady, vol.10, no.8, pp.707–710, 1966.
[6] A.S.J. Helberg and H.C. Ferreira, "On multiple insertion/deletion correcting codes," IEEE Trans. Inf Theory, vol.48, no.1, pp.305–308, 2002.
[7] G. Tenengolts, "Nonbinary codes, correcting single deletion or insertion," IEEE Trans. Inf. Theory, vol.30, no.5, pp.766–769, 1984.
[8] M.C. Davey and D.J. MacKay, "Reliable communication over channels with insertions, deletions, and substitutions," IEEE Trans. Inf. Theory, vol.47, no.2, pp.687–698, 2001.
[9] F. Wang, D. Fertonani, and T.M. Duman, "Symbol-level synchronization and LDPC code design for insertion/deletion channels," IEEE Trans. Commun., vol.59, no.5, pp.1287–1297, 2011.
[10] R. Goto, K. Kasai, and H. Kaneko, "Coding of insertion-deletion-substitution channels without markers," Proc. 2016 IEEE Int. Symp. Information Theory, pp.635–639, 2016.
[11] E. Arıkan, "Channel polarization: A method for constructing capacity-achieving codes for symmetric binary-input memoryless channels," IEEE Trans. Inf. Theory, vol.55, no.7, pp.3051–3073, 2009.
[12] E. Şaşoğlu, E. Telatar, and E. Arıkan "Polarization for arbitrary discrete memoryless channels," Proc. 2009 Information Theory Workshop, pp.144–148, 2009.
[13] I. Tal and A. Vardy, "List decoding of polar codes," IEEE Trans. Inf. Theory, vol.61, no.5, pp.2213–2226, 2015.
[14] E.K. Thomas, V.Y.F. Tan, A. Vardy, and M. Motani, "Polar coding for the binary erasure channel with deletions," IEEE Commun. Lett., vol.21, no.4, pp.710–713, 2017.
[15] K.D. Tian, A. Fazeli, and A. Vardy, "Polar coding for deletion channels: Theory and implementation," Proc. 2018 IEEE Int. Symp. Information Theory, pp.1869–1873, 2018.
[16] S. Kudekar, T.J. Richardson, and R.L. Urbanke, "Threshold saturation via spatial coupling: Why convolutional LDPC ensembles perform so well over the BEC," IEEE Trans. Inf. Theory, vol.57, no.2, pp.803–834, 2011.

Hikari Koremura received the B.E. and M.E. degrees in computer science both from Tokyo Institute of Technology, Japan, in 2017 and 2019, respectively. His research interests include polar coding for insertion, deletion, and substitution error correction.

Haruhiko Kaneko received the B.E., M.E., and Dr. Eng. degrees in computer science all from Tokyo Institute of Technology, Japan, in 1999, 2001, and 2004. He has been a post-doctoral research associate at Japan Aerospace Exploration Agency from 2004 to 2007. Since 2007, he has been an assistant professor at Tokyo Institute of Technology, and is now an associate professor. His research interests include error control coding and data compression for dependable high-performance computer systems. He received the FIT young researcher award and the IBM faculty award in 2008 and 2010, respectively. He is a member of IEEE Computer Society, IEEE Information Theory Society, IEICE Japan, and IPSJ.